doi: 10.3304/JMES.2017.001 *Journal of Mediterranean Earth Sciences 9 (2017), 5-17*

J M E S **Journal of Mediterranean Earth Sciences**

The Edough Massif garnetites: evidences for a metamorphosed paleo-garnet beach-sand placer (Cap de Garde, Annaba, Northeast Algeria)

Soraya Hadjzobir [a,*], Uwe Altenberger [b], Christina Günter [b]

[a] *Badji Mokhtar-Annaba University, Faculty of Earth Sciences, Laboratory of Soils and Sustainable Development, P.O. Box 12, 23000 Annaba, Algeria*

[b] *Institute of Earth and Environmental Science, University of Potsdam, Karl-Liebknecht-Strasse 24-25, D 14476 Potsdam-Golm Germany*

[*] *Corresponding author: shadjzobir@yahoo.fr*

ABSTRACT - Extremely garnet-rich metamorphic rocks occur at the "Cap de Garde", Ain Achir beach, Edough Massif, Algeria. Element distribution maps reveal that all garnets are zoned and most show conspicuous anhedral angular cores with significantly variable core compositions: these are in contrast to the chemically more homogeneous garnet mantling these cores. The cores are interpreted as clasts inherited from a previous metamorphic event different source rocks. After the erosion of garnet-bearing rocks and subsequent transport of the detrital grains, these garnet fragments and rounded staurolite formed part of a placer deposit, which was subsequently buried and metamorphosed. A comparison with the modern unconsolidated garnetite-rich placers (dark sands) near the studied outcrops at Ain Achir beach suggests that the garnetites have a protolith of clastic beach-sands or beach-placers deposits, particularly enriched in garnet fragments.

Mineral composition, abundance of different garnet varieties in some porphyroblasts and very similar rare earth element patterns of the metamorphosed sediments indicate that the garnets were derived from a similar source, i.e. a high-grade metamorphic gneiss series, prior to their later amphibolite facies metamorphic overprint. However, differences in the composition of the detrital cores reflect some differences in the source rock composition. The metamorphic growth of the garnet rims, which show oscillatory zoning, is probably influenced by fluids during a metasomatic event.

Key words: Garnetites, Provenance analysis; Beach-sand placers; Edough Massif; Algeria.

Submitted: 13 September 2016 - Accepted: 20 December 2016

1. INTRODUCTION

In the metamorphic, and metasedimentary series of the Edough massif, Algeria, rocks with extreme concentrations of garnet occur. These garnetites are composed of garnet embedded in a matrix composed of biotite and isometric grains of staurolite and quartz. These rocks can be classified as garnetites. Garnetites are metamorphic rocks, which are principally composed of up to 60% of garnets. They can form in many geological environments: such as restites of migmatized pelites in felsic plutons (e.g. Pett, 2006; Dorais and Tubrett, 2012; Dorais and Spencer, 2014), deep subduction zone environments (Selyatitskii and Reverdatto, 2014), by contact metamorphism or as metamorphosed placer deposits (Manzotti and Ballèvre, 2013). In addition, metamorphosed submarine hydrothermal activities (coticules, e.g. Kropáč et al., 2012) and metasomatic reactions between anatectic mafic and pelitic rocks can be responsible for the formation of garnetites (e.g. Spry et al., 2004). In the light of the neighbouring metasedimentary environment, we test the hypothesis of a placer deposit in contrast to a magmatic or hydrothermal origin. In this study we use bulk and mineral chemistry, as well as internal zonation morphologies in order to obtain evidence of the origin and evolution of these rocks. The results reveal the first occurrence of metamorphosed garnet-beach placers in the Edough Massif. This will give a tool for future paleogeographic reconstructions of the complete rock series. Hitherto, there is worldwide only one comparable occurrence described (Manzotti and Ballèvre, 2013).

2. GEOLOGICAL SETTING

The Edough Massif is an asymmetric metamorphic core complex exposed along the coastal region of Annaba north-east of Algeria. It is the easternmost crystalline massif of the Maghrebides, which comprise the southeastern part of the West Mediterranean orogen (Perrone et al., 2006;

Critelli et al., 2008). The core (Lower Unit) of the Edough Massif is composed of biotite gneiss and mica augen-gneiss of Hercynian age (Bruguier et al., 2009). These gneisses are altered diatexites and have arkosic protoliths (HadjZobir, 2012; HadjZobir and Mocek, 2012) and contain benches of leptynites and marbles (Hilly, 1962; Gleizes et al., 1988; Ahmed-Said et al., 1993), as well as ultramafic and mafic rocks (Bossière et al., 1976; Ahmed-Said and Leake, 1993, 1997; HadjZobir et al., 2007; HadjZobir and Oberhaensli, 2013) (Fig. 1). This "Lower Unit" is overlain by different types of micaschists (Caby et al., 2001) which are exposed in the northern part of the massif, mainly around the Cap de Garde. In these micaschists Gleizes et al., (1988) and Ahmed-Said and Leake (1992, 1995) have distinguished (i) a so called "Intermediate Unit" composed of garnet-staurolite-kyanite-micaschists alternating with marble layers. The contact between these two formations is formed by bimetasomatic skarns (reaction skarns), and (ii) the so called "Upper Unit" which consists of garnet-micaschists, garnet-andalusite-micaschists and alternating quartzites. Ahmed-Said and Leake (1995) suggest that these units were derived from illite-rich shales.

The sedimentary cover (not shown on the map) of the metamorphic massif is allochthonous. It is composed of several flysch deposits: (i) Cretaceous flysch, composed mainly of dark blue schistose argillite, and the Numidian formation of Oligo-Miocene age (Lahondère et al., 1979) that corresponds to a quartozose-sandstone formation with thin clay beds (Hilly, 1962). The metamorphic rocks and the sedimentary formations have been affected during Miocene (Langhian) by metamorphism owing to intrusions of high intrusions of high to intermediate acidic compositions (Fig. 1a).

The Edough Massif underwent a polymetamorphic evolution characterized by three major events: a high pressure granulite-facies event (HT-HP; P=12-13 kb, T=700 °C); followed by an amphibolite-facies event, and a low-pressure event at high temperature (LP-HT; P=3-4 kb, T=650-700 °C) (Brunnel et al., 1988; Ahmed-Said et al., 1993; Caby et al., 2001). The different metamorphic units underwent a first oblique deformation characterized by syn-metamorphic folds, followed by flexural shear generating upright folds of N140° direction, and anticlines with direction N50° to N60° with sense of shear ranging from N120° to N160°.

The 2 km^2 large study area (Cap de Garde) (Fig. 1b), which is a part of the Edough Massif, is located NE of the city of Annaba, Algeria and along the Mediterranean Sea. Metamorphic rocks consist of: andalusite-garnet-schists, kyanite-schists, staurolite-garnet-schists, marbles with some metamorphosed submarine basic ashes layers (HadjZobir et al., 2014), migmatic gneisses, reaction skarns, and garnetites. As part of the Edough massif, the rocks of the Cap de Garde experienced a polyphase regional metamorphism characterised by high-pressure (12-14 kbar) and medium-temperature metamorphic conditions (500-600 °C) (Brunnel et al., 1988; Ahmed-Said et al., 1993; Caby et al., 2001). The metamorphic grade increases from West (andalusite zone) to East (kyanite zone).

3. METHODS AND SAMPLING

The key to decipher the origin and evolution of minerals is its chemical composition, chemical variation and fabric. The present study is based on eight samples (1 garnet-micaschists, 1 staurolite-garnet micaschists, 1 garnet-quartzite and 5 garnetites). After examining thin sections of the rock samples for their mineralogical composition, samples were crushed and homogenized. 500 g splits were used for chemical analyses using XRF. Analyses for major and minor elements and for some trace elements were conducted on fused glass. Fused beads were prepared with a ratio of 1:6 between sample powder (<63 mm) and the melting agent FLUXANA FX-X 65-2 (99.98%) containing 66 wt% di-lithiumtetraborate and 34 wt% lithiummetaborate. Results were acquired by a Siemens SRS303-AS XRF with a Rh X-ray tube at standard running conditions at the GeoForschungsZentrum Potsdam (GFZ), Germany. Measurements of trace elements, including Nb, were performed in the ICP-MS laboratory at the (GFZ), using a VG Elemental Plasma Quad System PQ2+i. REE were analyzed at the GFZ laboratories by an ICP-OES (Varian Vista MPX) after separation of major and most trace elements. REE were enriched using the method described by Zuleger and Erzinger (1988). The instrument was calibrated with natural mineral standards. Detection limits varying with atomic number and range between 0.1 and 1.0 ppm.

To obtain information about the chemical analyses, zonation and internal fabrics of garnet and the element mapping were conducted using a fully automated JEOL JXA-8200 electron microprobe at laboratories of the Institute of Geosciences of the University of Potsdam, Germany. The instrument was calibrated with natural mineral standards.

We analyzed a total of 22 garnet grains in the following rock samples from the "Intermediate Unit": garnet quartzite HZ1 (2 grains), garnetites: HZ2 (4 grains), HZ3 (4 grains), HZ4 (4 grains), HZ5 (4 grains), HZ6 (4 grains). In each rock sample, garnets show similarities of the element distribution and the morphology of the zonation. Sometimes two rock samples have garnets with similar characteristics, for example garnets from sample HZ3 are similar to those from sample HZ2 and those from HZ5 to those samples HZ4. In our study we present four rock samples (1 garnet quartzite and 3 garnetites which are representative of the remaining 5) and their most representative garnets (HZ1: HZ grt1, HZ2: HZ2 grt4, HZ4: HZ4 grt2, HZ6: HZ6 grt3).

Major element profiles (CaO, FeO, MgO and MnO) were acquired along a linear traverse from rim to rim of the crystals. The structural formula of the analyzed garnets was calculated according to Locock (2008) (Tab. 2). X-ray element distribution maps were produced for garnets from four selected samples.

4. RESULTS: FIELD AND SAMPLE DESCRIPTIONS

4.1. Outcrops and petrography

The studied basement outcrops (Fig. 2a, 2c) at Achir beach are mainly composed of staurolite-garnet micaschists

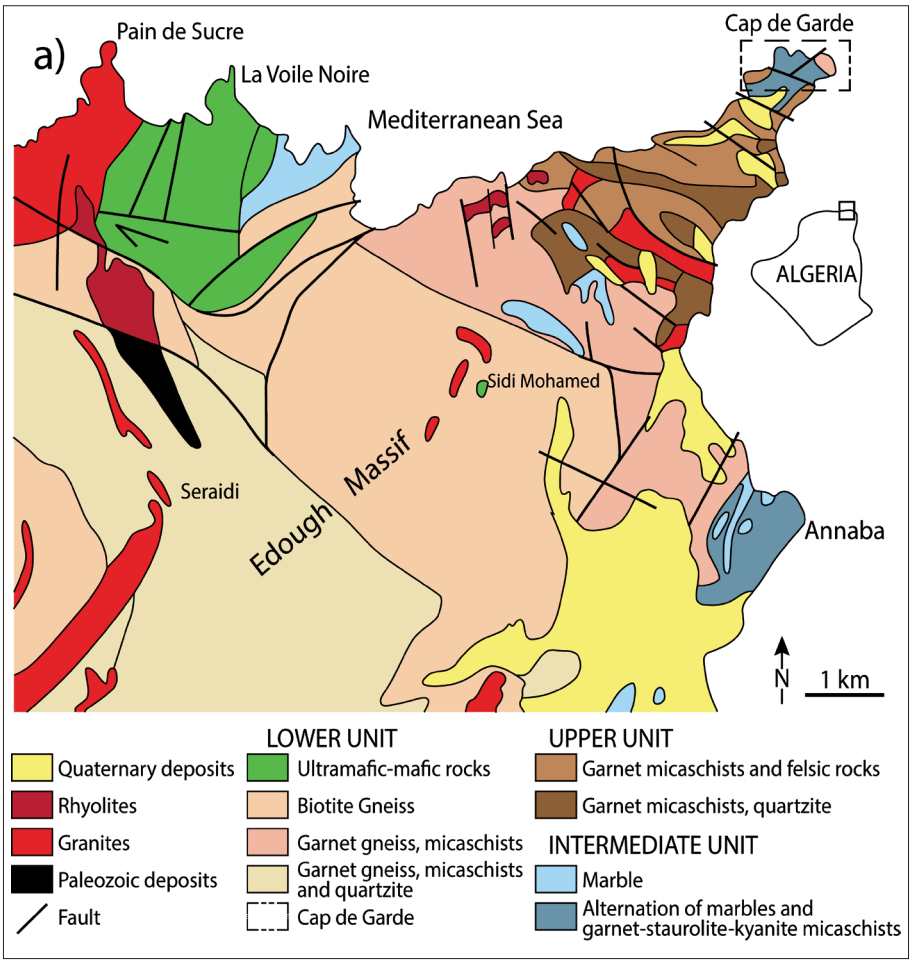

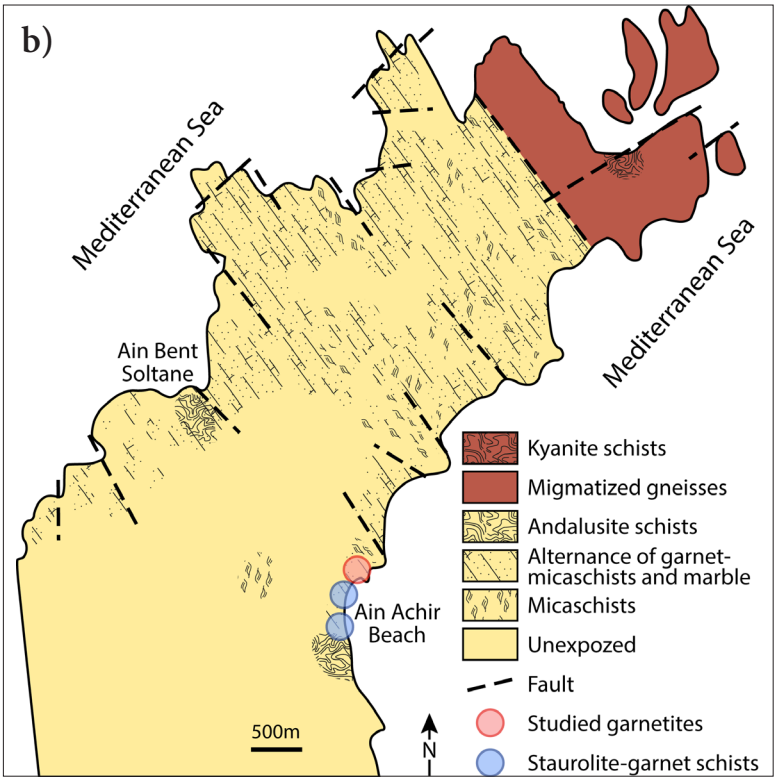

Fig. 1 - Simplified geological maps of: (a) the Edough massif modified after the works of Hilly (1962); SONAREM Project (1980); Gleizes et al. (1988); Caby and Hammor (1992); Ahmed-Said and Leake (1992, 1997); Hadjzobir et al., 2007, Hadjzobir, 2012; Hadjzobir et al. (2007); Hadjzobir (2012); Hadjzobir and Oberhaensli (2013); (b) Cap de Garde with the studied garnetites location.

(representative sample E74), garnet-quartzits (sample HZ) and garnetites. Nearby garnet-micaschists crop out (not shown) (sample E60). In addition, two kinds (light and dark) of modern, unsolidified beach sands (Fig. 2b) occur.

The staurolite-garnet micaschist layers (sample E74) are 2-10 m thick, massive and well foliated. Foliation is well defined by the shape-preferred orientation of muscovite and biotite. They are composed of fine-grained garnet, white mica, biotite, quartz and accessory staurolite (Fig. 3a). Garnet generally forms transparent, less than 1mm sized globular crystals that may have corroded rims. The garnet-micaschists (sample E60), have a very similar modal composition to the staurolite bearing schists, lacking staurolite (Fig. 3b).

The garnet-quartzite (sample HZ1) is from the contact zone (10-20 cm thick) between the staurolite-garnet micaschist layers and the garnetites. This zone is composed mainly of quartz, very rare staurolite and more garnet than in the staurolite-garnet micaschists. All garnets are in contact with biotite and occur as anhedral grains (0.06 cm). The garnets are mostly sub-rounded (Fig. 3c).

The garnetite layers are 10 to 40 cm thick and represented by the samples HZ2 to HZ6, which have been systematically collected across the area showing variable garnet grain size (0.18-1cm). Garnet grains are enclosed in a biotite, ± quartz, ± staurolite matrix (Fig. 3e, 3f). All the samples have similar mineral composition. Some of the garnets are euhedral, but many are quite anhedral. All garnets contain elongated ilmenite inclusions trails. Quartz is rare, less than 1 mm in diameter and occurs as elongated inclusions in the garnet and in the matrix. The regular distribution of these ilmenite

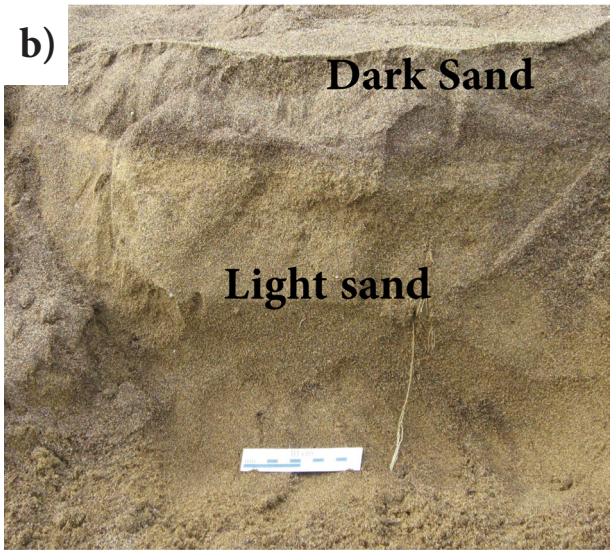

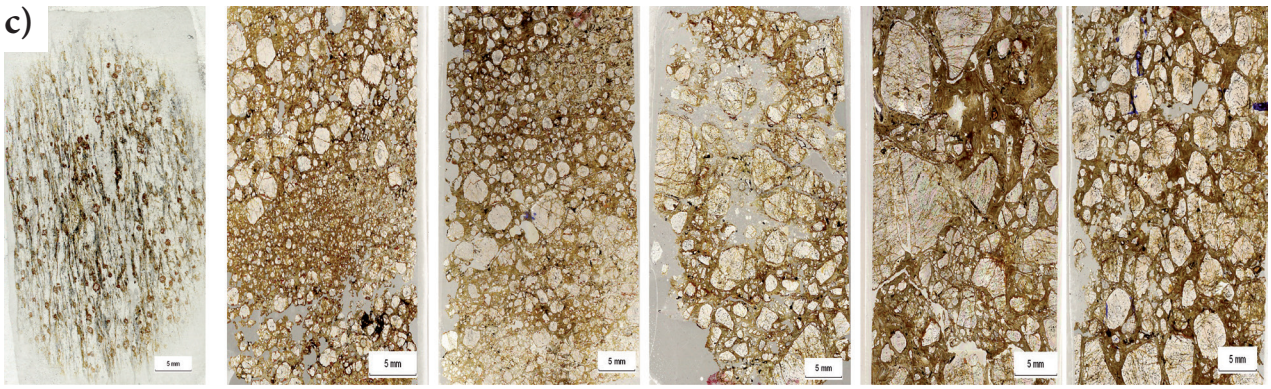

Fig. 2 - a) Garnetite outcrop, sandwiched between staurolite-garnet-micaschists; b) beach sand deposit in the modern Ain Achir sand showing light and dark sand near the garnetite, c) Scanned thin section showing the grain size evolution along the sampling transect from sample HZ1 to HZ6;

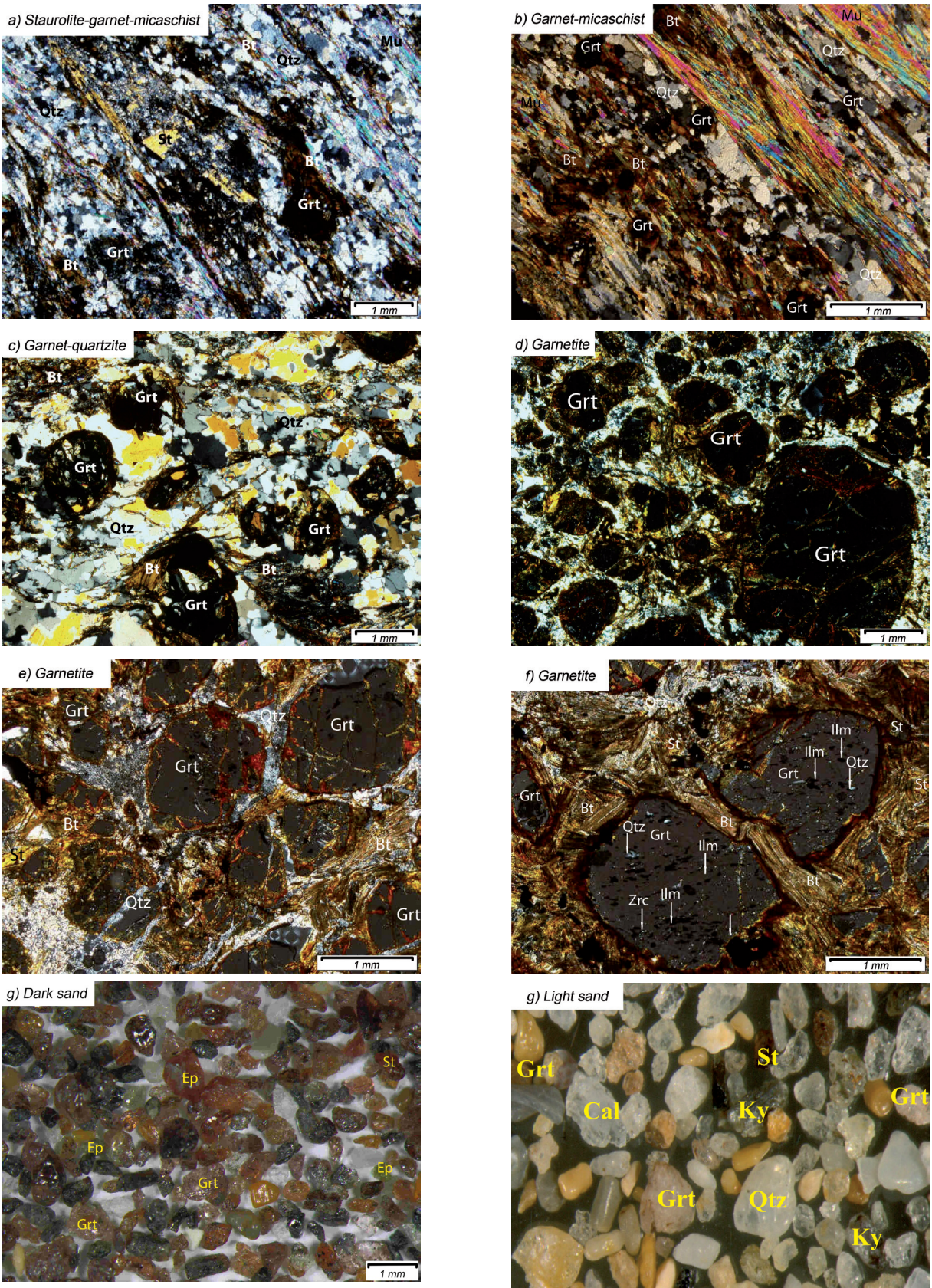

Fig. 3- a, b, c) Photomicrographs of the staurolite-garnet-micaschists (sample E74), garnet-micaschists (sample E60) and garnet-quartzite (HZ1) respectively; d-f) Photomicrographs of the garnetite; g-h) Recent dark and light garnet sand. Bt: biotite, Cal: calcite, Ep: epidote, Grt: garnet, Fsp: feldspar, Ilm: ilmenite, Ky: kyanite, Mnz: monazite, Ms: muscovite, Qtz: quartz, St: staurolite, Tur: tourmaline, Zrn: zircon (abbreviations are after Whitney and Evans, 2010).

inclusions in trails and their symmetrical arrangement in different porphyroblasts indicate that these inclusions are related to the growth zoning in the garnets. Accessories are rutile, zircon and monazite (Fig. 3f).

The modern Ain Achir sand beach is often dark in colour, but after sea storm, light sand occurs, too. The dark sand is composed by up to 60% of heavy minerals, such as (garnet, tourmaline, kyanite, biotite and epidote). Most of the dark grains have angular and sharp contours (Fig. 3g). The light sand contain 70 vol% light grains: feldspar, muscovite, calcite and deformed quartz grains as is displayed by undulose extinction. Other minerals are relatively minor (30 vol%) and include metamorphic minerals such as garnet, kyanite and staurolite (Fig. 3h). The density contrast between the heavy and light grains allows the hydraulic segregation of the components, by sea wave action, producing a heavy-mineral-placer deposit.

4.2. Whole rock composition

In order to determine the relationship between the garnetites and its adjacent rocks (the garnet-staurolite micaschists and the garnet-quartzite) the bulk rock composition of eight samples was analyzed (Tab. 1). The composition of the garnet-staurolite micaschists (sample E74) and garnet-quartzite (sample HZ1) shows only small differences. Both rock types are characterized by high SiO_2 (up to 71 wt.%). FeO_{tot} and K_2O are higher in the garnet-micaschists, (sample E60) reflecting its higher modal composition in biotite content than in the garnet-staurolite-micaschists. In the latter sample, the concentration of the alkalies and aluminium are slightly higher than in sample HZ1 (garnet-quartzite), pointing to a larger feldspar content. The garnet-staurolite-micaschists have a very high SiO_2 and the lowest aluminium and alkalies concentration, as a consequence of their quartz rich and feldspar-poor composition. In contrast, the garnetites reveal a significant low concentration of SiO_2 (» 34 wt%) and high concentrations of FeO_{tot} (» 34 wt.%) and MgO (» 4-5 wt.%). CaO is low (<1 wt.%) and K_2O ranges from 1.0-1.5 wt.%. All analyzed garnetites have very similar chemical compositions, except the varying concentration in TiO_2 (0.87-2.61 wt.%) and in P_2O_5 (0.13-0.49 wt.%). The high values of TiO_2 and P_2O_5 are due to the presence of abundant ilmenite and apatite inclusions in the garnets (Fig. 3f).

The total concentration of rare earth elements (REE) in the garnetites varies from 151 to 387 ppm. However, they are significantly higher than in the different neighbouring formations (82-217 ppm). The garnetites have mostly higher light REE (LREE) as well as heavy REE (HREE) concentrations than the micaschists. Apart from sample HZ6, La/Yb ratios in the garnetites are very similar varying from 28 to 30. The garnet-quartzite has higher La/Yb ratios (29) than the garnet-staurolite-micaschists (15) and the garnet-micaschists (10). After normalization to continental crust (after Rudnick and Gao, 2003) the garnetites show $(La/Yb)_n$ ratios significantly higher than 1 although garnets are the major constituents and ratios <1 are expected (Harley and Kelly, 2007) (Fig.4). Consequently, a LREE-rich phase must be responsible for this pattern. The garnetites have significantly higher P_2O_5 (0.13-0.49 wt.%) and CaO (0.58-0.82 wt.%) concentrations than the micaschists (P_2O_5= 0.04-0.1 wt % and CaO=0.11-0.26 wt.%). Therefore, apatite and monazite are probably responsible for the increase in LREE and La/Yb-ratios. The REEs concentration in staurolite (<5 ppb) and biotite (<1ppm) are commonly below the detection limits of the LA-ICP-OES and -MS (Corrie and Kohn, 2008). The significant negative Eu anomaly of all samples, if normalized to continental crust, indicates the

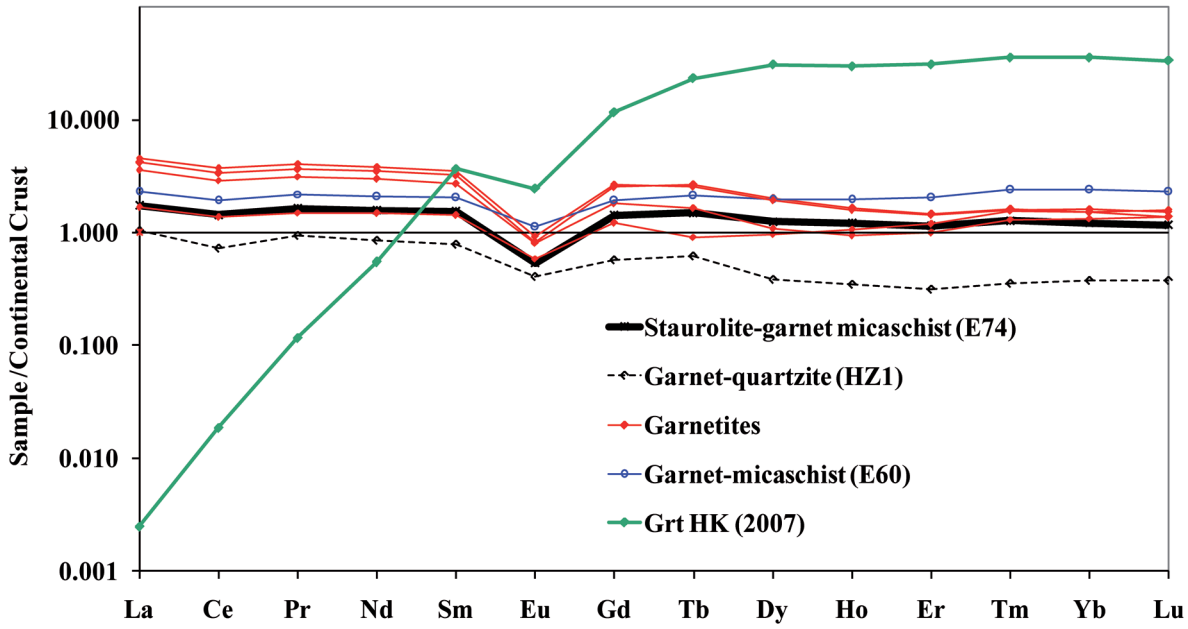

Fig. 4 - REE distribution pattern for whole-rock sample of Ain Achir garnetites compared with the pattern of staurolite-garnet-micaschists (E74), Garnet-quartzite (HZ1) and garnet-micaschists (E60) and an almandine rich garnet (Grt HK 2007) from Harley and Kelly (2007).

paucity of plagioclase in the protoliths and therefore in the metamorphic equivalents, too. The other high field strength elements like Nb, Y and Sc are enriched in garnetites (Nb: 18-45ppm, Y:19-29 ppm and Sc:17-24 ppm) compared to the garnet-quartzite (HZ1: Nb: 10 ppm, Y:6 ppm and Sc: 4.13 ppm) and the nearby garnet-staurolite micaschists unit (E74: Y: 22ppm and Sc: 10.58 ppm) (Tab. 1). This is probably due to their high content of garnet which concentrates these elements.

	Garnet micaschist	Garnet-staurolite micaschist	Garnet quartzite	Garnetites				Garnet (Harley and Kelly 2007)
Samples	E60	E74	HZ1	HZ 2	HZ3	HZ4	HZ6	
SiO_2	66.22	71.00	81.11	34.69	34.35	34.82	33.75	
TiO_2	0.16	0.76	0.37	0.87	1.23	1.64	2.61	
$Al2O_3$	17.34	14.01	6.22	18.61	18.46	18.84	18.29	
Fe_{tot}	5.79	5.04	8.53	34.38	34.13	34.15	32.98	
MnO	0.05	0.03	0.03	0.12	0.12	0.16	0.12	
MgO	1.00	1.06	1.15	4.05	4.32	4.46	4.99	
CaO	0.11	0.26	0.16	0.64	0.71	0.58	0.82	
Na_2O	0.35	0.30	0.24	0.35	0.21	0.35	0.24	
K_2O	3.66	3.35	0.41	1.02	1.23	1.11	1.50	
P_2O_5	0.08	0.10	0.04	0.15	0.13	0.26	0.49	
LOI	3.90	3.40	1.56	4.75	4.93	3.29	3.98	
Total	98.66	99.32	99.83	99.63	99.81	99.67	99.77	
Cr	220.00	260.00	39.00	118.00	138.00	219.00	295.00	
Zr	455.00	383.00	192.00	149.00	246.00	201.00	210.00	
Sr	73.00	32.00	13.00	10.00	12.00	16.00	27.00	
Zn	137.00	87.00	36.00	61.00	71.00	69.00	86.00	
Ni	270.00	242.00	28.00	85.00	105.00	102.00	155.00	
Ba	457.00	100.00	47.00	69.00	36.00	35.00	38.00	
Rb	226.00	465.00	17.00	33.00	32.00	30.00	19.00	
Nb	nd	nd	10.00	18.00	25.00	37.00	45.00	
Sc	46.11	10.58	4.13	19.73	24.17	17.01	17.54	
Y	37.20	22.51	6.37	29.07	27.52	19.41	19.72	
La	46.11	34.78	20.74	83.88	91.49	71.62	33.59	0.05
Ce	82.41	61.78	31.37	144.89	158.93	124.39	59.10	0.80
Pr	10.73	8.07	4.61	18.07	19.65	15.33	7.37	0.57
Nd	41.71	31.42	17.01	70.06	76.29	59.90	29.75	10.93
Sm	8.01	6.04	3.04	12.54	13.61	10.53	5.58	14.38
Eu	1.24	0.59	0.45	0.91	1.01	0.89	0.65	2.69
Gd	7.16	5.26	2.14	9.42	9.84	6.74	4.52	43.00
Tb	1.27	0.90	0.37	1.59	1.53	0.98	0.55	14.00
Dy	7.09	4.49	1.37	7.23	6.90	3.89	3.48	111.00
Ho	1.52	0.94	0.27	1.26	1.22	0.72	0.82	23.00
Er	4.27	2.40	0.66	3.07	2.98	2.10	2.51	65.00
Tm	0.67	0.36	0.10	0.45	0.45	0.37	0.44	10.00
Yb	4.53	2.31	0.71	2.89	3.05	2.52	2.91	68.00
Lu	0.69	0.35	0.11	0.41	0.46	0.41	0.47	10.00
SREE	217.41	159.68	82.95	356.66	387.39	300.40	151.73	373.42
La/Yb	10.18	15.07	29.05	28.99	30.02	28.39	11.53	0.001

Tab. 1 - Whole rock and almandine rich garnet (Harley and Kelly, 2007) composition. Majors elements are in wt%, trace elements including REE elements are listed in ppm; nd: not determined.

4.3. Garnet composition

Electron microprobe analyses of the garnets show significant variations in chemical composition from core to rim, indicating that some garnets are zoned (Tab. 2).

Garnet from garnet-quartzite (HZ1):

The an- to subhedral garnet grain (sample HZ1grt1) is chemically nearly unzoned. However, a small core, less than 100µm in diameter, has significantly higher CaO and lower MgO concentrations. (Figs. 5a, 6a, Tab. 2). The MnO and FeO profiles are flat. Composition varies significantly for Ca and Fe, expressed by the different proportions of components, changing from $Alm_{78}Prp_{14}Sps_{0.5}Grs_{7}$(core) to $Alm_{84}Prp_{14}Sps_{0.5}Grs_{1}$ (rim) (Tab. 2).

Garnets from garnetites:

Garnet HZ2grt4: is one of the few euhedral grains in this sample. The element map displays a strong chemical difference between a central angular core and the adjacent rim. The core is strongly enriched in Mn and Ca and depleted in Fe and Mg in contrast to the broad rim (Figs. 5b, 6b, Tab. 2). The compositional jump led from $Alm_{69}Prp_{2}Sps_{5}Grs_{24}$ (core) to $Alm_{78}Prp_{20}Sps_{01}Grs_{1}$(rim) (Tab. 2). Zoning of the broad rim is more complex (Fig. 6b), as shown by the fluctuations in the CaO. The oscillatory zoning of Ca reflects a probable change in PT-conditions of the mantle and implies that this garnet did not homogenise during growth.

The studied garnet of sample HZ4grt2 shows two distinct growth zones. The first one (zone 1) is localized in the top left edge of the grain as portrayed in Figure 6c. This rectangular "core" differs with high Mn and low Ca but similar Mg and Fe concentrations compared to the second zone. Zone 2 which covers the whole central and lower part (according to Figure 6c) shows a chemical zoning with increasing Mg, Ca and Mn from core to rim and a weakly decreasing Fe concentrations (Figs. 5c, 6c, Tab. 2).

	Garnet-quarzite		Garnetites					
	HZ1grt1	HZ1grt1	HZ2grt4	HZ2grt4	HZ4grt2	HZ4grt2	HZ6grt3	HZ6grt3
	core	rim	core	rim	core	rim	core	rim
SiO_2	38.04	38.06	36.42	38.72	36.91	37.95	37.14	38.13
TiO_2	0.07	0.04	0.11	0.03	0.02	0.01	0.18	0.03
Al_2O_3	21.57	21.39	21.79	21.93	21.25	22.03	20.96	21.65
FeO	34.93	36.95	30.91	35.1	39.95	34.05	36.52	34.78
MnO	0.14	0.2	2.1	0.04	0.07	0.16	1.78	0.07
MgO	3.5	3.42	0.45	5.04	1.9	5.42	0.99	5.18
CaO	2.57	0.44	8.66	0.42	0.2	0.61	2.77	0.58
Cr_2O_3	0.01	0.02	0.07	0.02	0.14	0.03	0.03	0.11
Total	100.83	100.52	100.52	101.3	100.44	100.26	100.37	100.53
Si	6.02	6.06	5.86	6.05	5.98	5.98	6.02	6.01
Ti	0.01	0	0.01	0	0	0	0.02	0
Al	4.02	4.02	4.13	4.04	4.06	4.09	4	4.02
Fe	4.62	4.92	4.16	4.59	5.41	4.49	4.95	4.59
Mn	0.02	0.03	0.29	0.01	0.01	0.02	0.24	0.01
Mg	0.83	0.81	0.11	1.17	0.46	1.27	0.24	1.22
Ca	0.44	0.08	1.49	0.07	0.03	0.1	0.48	0.1
Cr	0	0	0.01	0	0.02	0	0	0.01
Total	15.96	15.92	16.05	15.92	15.96	15.96	15.95	15.95
Alm(%)	78.31	84.34	68.54	78.59	91.49	76.25	83.69	77.59
Prp(%)	13.99	13.91	1.8	20.11	7.76	21.63	4.04	20.6
Sps(%)	0.32	0.46	4.77	0.09	0.16	0.36	4.13	0.16
GAU(%)	7.38	1.29	24.89	1.2	0.59	1.75	8.13	1.66
Total	100	100	100	100	100	100	100	100
Grs(%)	99.76	99.82	98.35	99.85	99.5	99.88	99.36	99.57
Adr(%)	0.21	0.12	1.44	0.09	0.06	0.03	0.54	0.09
Uva(%)	0.03	0.06	0.22	0.06	0.44	0.09	0.1	0.34
Total	100	100	100	100	100	100	100	100

Tab. 2 - Representative electron microprobe analyses of garnets from the Cap de Garde garnetites, GAU: grossular-andradite-uvarovite.

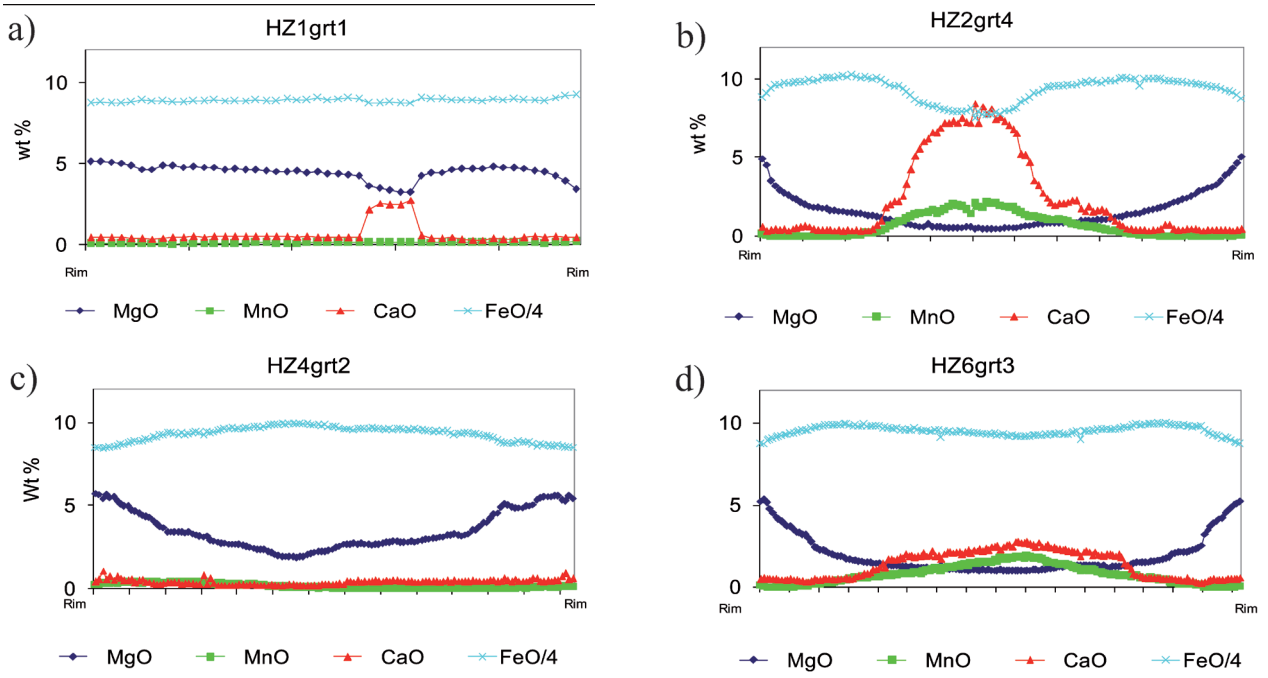

Fig. 5 - Rim-rim profiles of Mg, Mn, Ca and Fe components in garnets from: a) sample HZ1 (Garnet-quartzite) and b, c, d) the garnetites samples.

Garnet HZ6grt3: The element profiles and maps of this garnet reveal a very similar zoning as for sample HZ2grt4. (Figs. 5b, 6b). An angular-shaped Ca-and Mn-rich and Mg-poor core is in strong contrast to the composition of the rim. The garnet composition changes strongly from $Mg_{0.24}$ to $Mg_{1.22}$ and from $Ca_{0.48}$ to $Ca_{0.1}$.

5. DISCUSSION

5.1. Metamorphic evolution

Metamorphic grade and metamorphic evolution might be inferred from garnet composition. (e.g. Win et al., 2007; Andò et al., 2014). The presence of breaks and gaps in the zoning trends of the garnet suggests that they had a discontinuous and irregular growth as a result of a multistage evolution. The lack of a significant zoning of the major elements (e.g. garnet HZ1grt1 from the garnet-quartzite sample HZ1) suggests homogenization at high temperatures during or/after growth. The occurrence of garnet cores of significantly different composition in the outcrop of garnetites confirms that the garnets grew during various metamorphic conditions. Chemical discrimination diagrams, based on garnets with known pressure and temperature conditions of formation and rock environment (Méres and Hovorka, 1991; Méres, 2008; Aubrecht et al., 2009) (Fig. 7a) are used to delimit the formation conditions. All the garnet cores indicate an origin from gneisses metamorphosed under transitional or granulite- and amphibolite-facies conditions. In addition, the plots of the studied garnets in the ternary discrimination diagram after Mange and Morton (2007) (Fig. 7b) show that the cores of the garnets from the garnetites grew under amphibolite-facies conditions, whereas the rims grew at granulite- and amphibolite-facies conditions. The preservation of different garnet core compositions in one outcrop or layer point to the detrital origin of these cores from different source rocks. Furthermore, the occurrence of zoned garnets with a (detrital) core and a rim formed at different metamorphic conditions and garnets with (non-detrital) core and rim formed at similar metamorphic conditions supports this hypothesis.

5.2. Source rocks and provenance-a discussion

The presence of bimetasomatic skarns near to the outcrops of the studied samples and the unusual high concentrations of incompatible elements e.g., Rb, Ba and heavy metals e.g., Zn of the garnet-micaschists (E60) and garnet-staurolite micaschists (E74), and the low concentrations of Rb and Ba in the garnetites, gives evidence for a fluid-controlled and/or metasomatic processes. The garnets of the garnetites show oscillatory zoning in the mantles of the detrital cores (Fig. 5). Yang and Rivers (2001) pointed out that oscillatory zoning in metamorphic minerals is common in fluid/metasomatic dominated environments. The garnet sample HZ2grt4 show Mn, Ca and Mg oscillatory zoning (Fig. 5b), whereas Mg oscillatory is pronounced in sample HZ4grt2 (Fig. 5c) and Ca oscillatory zoning in sample HZ6grt3 (Fig. 5d).

Figure 8 shows also evidence of fluid-controlled and/or metasomatic processes in a fragmented garnet grain from the garnetite sample. The similar Mg content of core (1) corresponds to a primary growth before breaking. The similar Mg content increase from rim (2) to rim (3) in each grain part can be interpreted as a secondary zoning growth after fracturing. The secondary zoning and the monotonous increase of Mn towards the new rims (1 and 2) indicate a chemical exchange between the rock matrix and the fracture surface.

All examined garnetite samples contain garnets that preserve chemical zoning with variable degrees (Fig. 6).

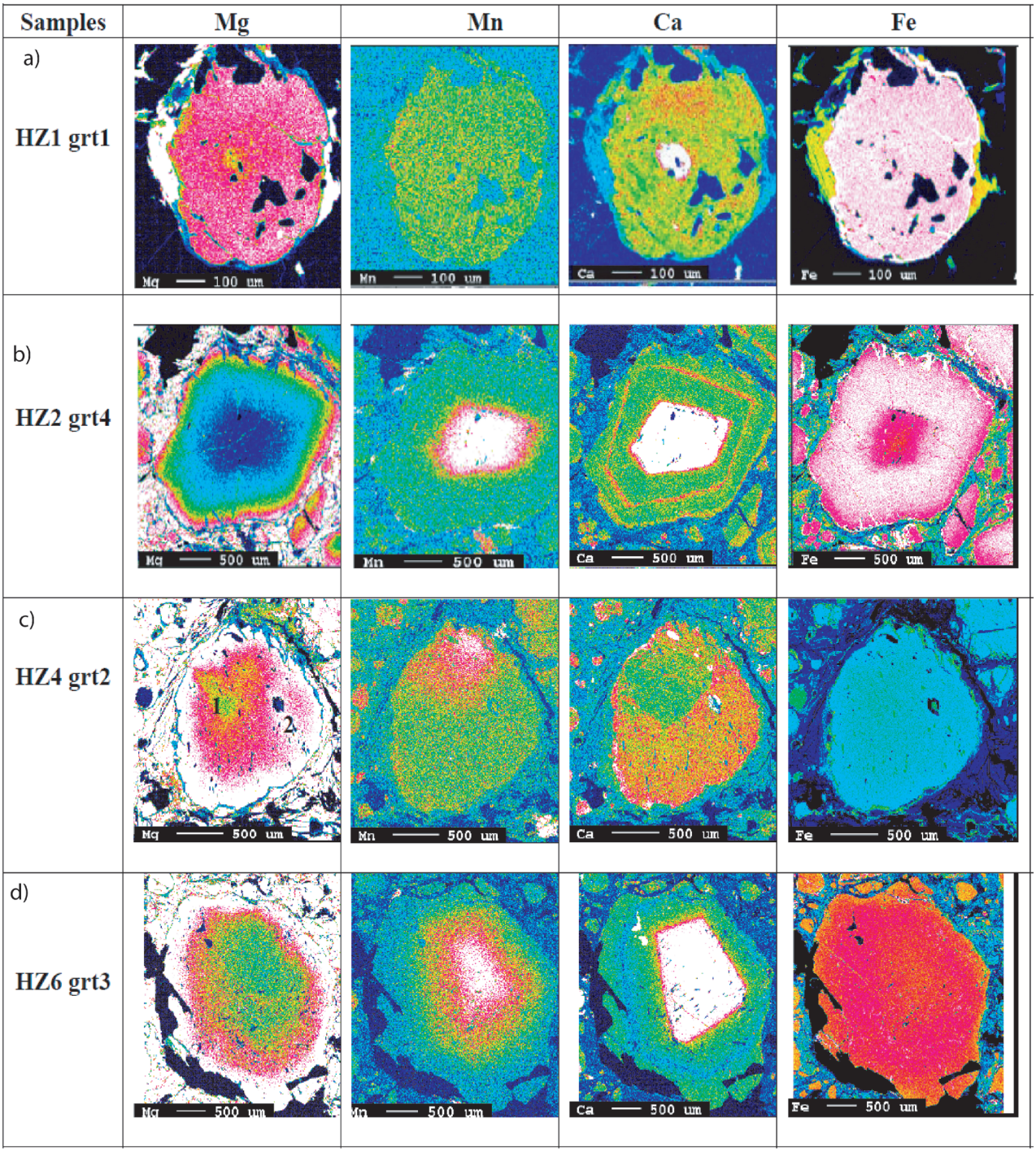

Fig. 6 - Compositional maps in garnet from selected samples: HZ1 (Garnet-quartzite) and HZ2-HZ6 (garnetites). Element concentration colour scale- White: very high, red: high, green: moderate, blue: low.

In contrast to oscillating or continuous zoning profiles, most of the samples show an abrupt and strong chemical contrast between the angular (Fig. 6b), often rectangular core, and the broad rim (garnet sample HZ6grt3) (Fig. 6d). Especially the shape from these angular and rectangular cores remembers garnet fragments, i.e. detrital grains. Therefore, the form and "jump" in chemical composition make an interpretation as overgrown detrital garnets very likely. The staurolite-garnet micaschists (E74) and garnet-micaschists (E60) are characterized by its aluminium- and silica-rich whole-rock compositions and by the presence of staurolite, pointing to a metasedimentary origin, too. The garnet-quartzite with its low concentration in alkalies pointing to a feldspar-depleted quartz-sand as a protolith. The direct vicinity of the quartzite, i.e. former metamorphosed quartz-sand and the garnetites i.e. metamorphosed heavy mineral sand, indicate a sedimentary selection process.

Continental-crust-normalized REE patterns (after Rudnick and Gao, 2003) (Fig. 4) show LREE enrichment and near continental crust HREE values for the staurolite-rich and poor-garnet micaschists (E74) and the garnetites. Whereas the garnet-quartzite sample (HZ1) is slightly depleted in

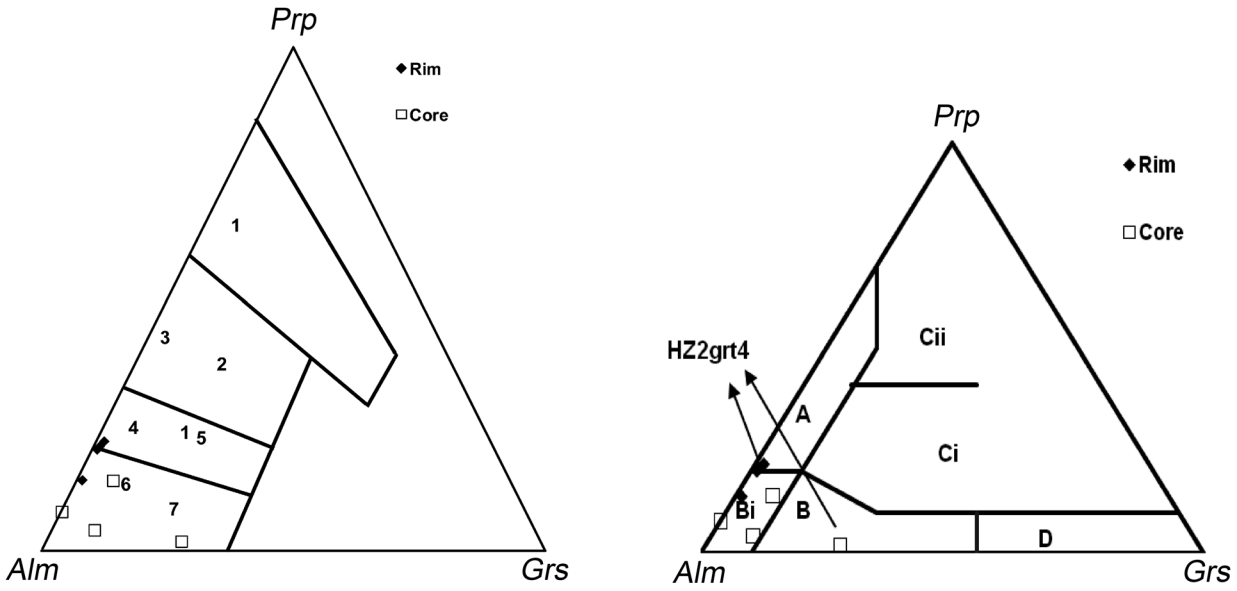

Fig. 7 - **(a)** Ternary discrimination diagram after Méres and Hovorka (1991), Méres (2008) and Aubrecht et al (2009). 1- garnets derived from UHP garnet peridotites, 2- garnets derived from HP mafic granulites, 3- garnets derived from felsic and intermediate granulites, 4- garnets derived from gneisses metamorphosed under granulite- and amphibolite-facies conditions, 5- garnets derived from amphibolites metamorphosed under granulite- and amphibolite-facies conditions, 6- garnets derived from gneisses metamorphosed under amphibolite-facies conditions, 7- garnets derived from amphibolites metamorphosed under amphibolite-facies conditions; **(b)** ternary discrimination pyrope-almandine-grossular diagram after Mange and Morton (2007). A- from high-grade granulite-facies metasediments and intermediate felsic igneous rocks, B- amphibolite-facies metasedimentary rocks, Bi- intermediate to felsic igneous rocks, Ci- from high-grade mafic rocks, Cii- ultramafics, -metasomatic rocks, very low-grade metamafic rocks and ultrahigh temperature metamorphosed calc-silicate granulites.

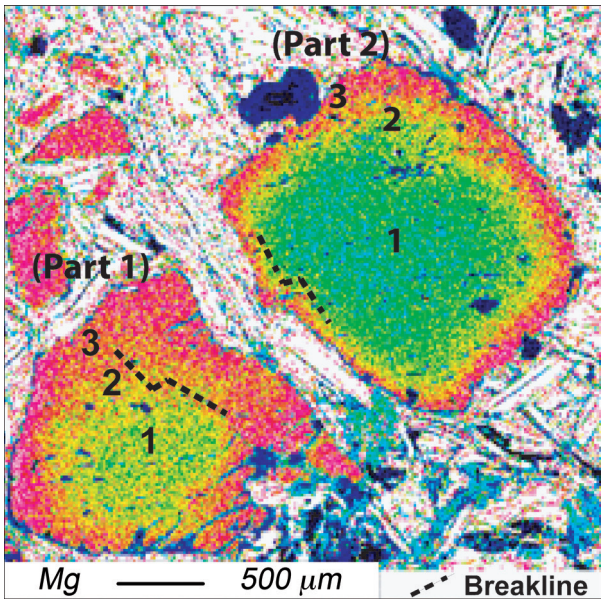

Fig. 8 - Compositional maps of two grain parts of a broken garnet, indicating fluid circulation and multiple metamorphic and/or metasomatic events during growth.

REE, all other samples have very similar and flat REE patterns, suggesting that they have similar source rocks. In comparison to the average continental-crust, the HREE concentrations of the garnet-micaschists sample (E60) are significantly high. The newly-formed metamorphic minerals of the analyzed samples and the possible inherited detrital grains (garnets with angular-shaped core) control largely the REE pattern. As shown earlier, the high HREE continental crust-normalized concentrations reflect the contribution of garnets. The high continental crust-normalized LREE concentrations are due to the existence of monazite. This mineral is known to occur as inherited detrital grains, partly overgrown by metamorphic rims (e.g. Kohn et al., 2005). The negative Eu-anomaly is probably due to the instability of plagioclase during weathering and/or an Eu-poor source like K-feldspar-rich granitoid (e.g. Borrelli et al., 2012, 2014; Scarciglia et al., 2016). In a possible scenario, the garnetites yield evidence of eroded garnet-staurolite bearing micaschists located nearby, similar to the recent situation at the beach of the sample area (Fig. 2c). Here, garnet placers are interlayered with light sands.

6. CONCLUSIONS

The garnet composition, the abundance of different garnet varieties in some porphyroblasts, the very similar REE patterns of the garnetites, the staurolite-garnet micaschists, garnet-micaschists and the garnet-quartzite permit to conclude that the garnets were derived from similar source rocks, i.e. high-grade metamorphic gneisses. All samples show the same conspicuous angular garnet cores with strong chemical contrast to their large rims. These cores can be interpreted as relict clasts of sediments. Therefore the "Cap de Garde" garnetites are metamorphic

rocks derived from clastic sediments enriched in garnet fragments like beach-sands or beach-placers. Beach placer deposits are known for heavy minerals such as ilmenite, tourmaline, zircon, monazite, staurolite and garnet. These mineral grains are derived from the weathering of pre-existing rocks and deposited as beach sands. The nearby modern sands (light and dark one) at the Ain Achir beach are an analogue to the garnet-quartzite (light sand) and the garnetites (dark sands).

ACKNOWLEDGEMENTS - We thank C. Fischer, A. Musiol and B. Fabian from Potsdam University and the GFZ (German Research Center for Geosciences) for their support in sample preparation and analytical laboratories. The first author also thanks Badji Mokhtar-Annaba University for financial support. We also acknowledge the reviewers S. Critelli and D. Tentori whose comments greatly improved the manuscript.

REFERENCES

Ahmed-Said Y., Leake B.E., 1992. The composition and origin of Kef Lakhal amphibolites and associated amphibolite and olivine-rich enclaves, Edough, Annaba, NE Algeria. Mineralogical Magazine 56, 459-468.

Ahmed-Said Y., Leake B.E., Rogers G., 1993. The petrology, geochemistry and petrogenesis of the Edough igneous rocks, Annaba, NE Algeria. Journal of African Earth Sciences 17, 111-123.

Ahmed-Said Y., Leake B.E., 1995. The petrogenesis of the Edough orthogneisses, Annaba, northeast Algeria. Journal of African Earth Sciences 21, 253-269.

Ahmed-Said Y., Leake B.E., 1997. The petrogenesis of the Edough amphibolites, Annaba, NE Algeria; two unrelated basic magmas and the lherzolite-harzburgite residue of a possible magma source. Mineralogy and Petrology 59, 207-237.

Andò S., Morton A., Garzanti E., 2014. Metamorphic grade of source rocks revealed by chemical finger prints of detrital amphibole and garnet. In: Scott R.A., Smyth H.R., Morton A.C., Richardson N. (Eds.), Sediment Provenance Studies in Hydrocarbon Exploration and Production. Geological Society, London, Special Publications 386, 351-371.

Aubrecht R., Méres Š., Sýkora M., Mikus T., 2009. Provenance of the detrital garnets and spinels from the Albian sediments of the Czorsztyn Unit (Pieniny Klippen Belt, Western Carpathians, Slovakia). Geologica Carpathica 60, 463-483.

Borrelli L., Perri F., Critelli S., Gullà G., 2012. Minero-petrographical features of weathering profiles in Calabria, southern Italy. Catena 92, 196-207.

Borrelli L., Perri F., Critelli S., Gullà G., 2014. Characterization of granitoid and gneissic weathering profiles of the Mucone River Basin (Calabria, southern Italy). Catena, 113, 325-340.

Bossière G., Collomb P., Mahdjoub Y., 1976. Sur un gisement de Péridotites découvert dans le massif cristallophyllien de l'Edough (Annaba, Algérie). Comptes Rendus Géoscience 283, 885-888.

Bruguier O., Hammo D., Bosch D., Caby R., 2009. Miocene incorporation of peridotite into the Hercynian basement of the Maghrebides (Edough massif, NE Algeria): Implications for the geodynamic evolution of the Western Mediterranean. Chemical Geology 261, 172-184.

Brunnel M., Hammor D., Misseri M., Gleizes G., Bouleton J., 1988. Cisaillements synmétamorphes avec transport vers le Nord-Ouest dans le massif cristallin de l'Edough (Est Algérien). Comptes Rendus Géoscience 306, 1039-1045.

Caby R., Hammor D., 1992. Le Massif cristallin de l'Edough (Algérie): un " Métamorphic Core Complex" d'âge miocène dans les Magrébides. Comptes Rendus Géoscience 314, 829-835.

Caby R., Hammor D., Delor C., 2001. Metamorphic evolution, partial melting and Miocene exhumation of lower crust in the Edough metamorphic core complex, west Mediterranean orogen, eastern Algeria. Tectonophysics 342, 239-273.

Corrie S.L., Kohn M.J., 2008. Trace-element distributions in silicates during prograde metamorphic reactions: implications for monazite formation. Journal of Metamorphic Geology 26, 451-464.

Critelli S., Mongelli G., Perri F., Martin-Algarra A., Martin-Martin M., Perrone V., Dominici R., Sonnino M., Zaghloul M.N., 2008. Sedimentary evolution of the middle Triassic -lower Jurassic continental redbeds from western-central Mediterranean Alpine chains based on geochemical, mineralogical and petrographical tools. Journal of Geology 116, 375-386.

Dorais M.J., Tubrett M., 2012. Detecting Peritectic Garnet in the Peraluminous Cardigan Pluton, New Hampshire. Journal of Petrology 53, 299-324.

Dorais M.J., Spencer C.J., 2014. Revisiting the importance of residual source material (restite) in granite petrogenesis: The Cardigan Pluton, New Hampshire. Lithos 202, 237-249.

Gleizes G., Bouloton J., Bossière G., Collomb P., 1988. Donneés lithologiques et pétro-structurales nouvelles sur le massif cristallophyllien de l'Edough (Est-Algérie). Comptes Rendus de L' Academie Des Sciences 306, 1001-1008.

HadjZobir S., 2012. Impact de l'altération sur le bilan chimique des diatexites du massif de l'Edough (Annaba, NE Algérien) Estudios Geologicos 68, 203-215.

HadjZobir S., Mocek B., 2012. Determination of the source rocks for the diatexites from the Edough Massif (Annaba, NE Algeria). Journal of African Earth Sciences 69, 26-33.

HadjZobir S., Oberhaensli R., 2013. The Sidi Mohamed peridotites (Edough Massif, NE Algeria): Evidence for an upper mantle origin. Journal of Earth System Science 122, 1455-1465.

HadjZobir S., Laouar R., Oberhaensli R., 2007. Les métabasites de Sidi Mohamed Edough NE Algérien Caractéristiques pétrographiques minéralogiques et géochimiques. Service Géologique National 18, 25-41.

HadjZobir S., Altenberger U., Günter C., 2014. Geochemistry and petrology of metamorphosed submarine basic ashes in the Edough Massif (Cap de Garde, Annaba, northeastern Algeria). Comptes Rendus Géoscience 346, 244-254.

Harley S.L., Kelly N.M., 2007. The impact of zircon-garnet REE distribution data on the interpretation of zircon U-Pb ages in complex high-grade terrains: An example from the Rauer Islands, East Antarctica. Chemical Geology 241, 62-87.

Hilly J., 1962. Etude géologique du massif de l'Edough et du Cap de Fer (Est-Constantinois). Bulletin du Service de la carte

géologique de l'Algérie 19, 1-408

Kohn M.J., Wieland M.S., Parkinson C.D., Upreti B.N., 2005. Five generations of monazite in Langtang gneisses: implications for chronology of the Himalayan metamorphic core. Journal of Metamorphic Geology 23, 399-406.

Kropáč K., Buriánek D., Zimák J., 2012. Origin and metamorphic evolution of Fe–Mn-rich garnetites (coticules) in the Desná Unit (Silesicum, NE Bohemian Massif). Chemie der Erde - Geochemistry 72, 219-236.

Lahondère J.C., Feinberg H., Haq B.U., 1979. Datation des grès numidiens d'Algérie orientale: conséquences structurales. Comptes Rendus de l'Académie des Sciences 289, 383-386.

Locock A.J., 2008. An Excel spreadsheet to recast analyses of garnet into end-member components, and a synopsis of the crystal chemistry of natural silicate garnets. Computers and Geosciences 34, 1769-1780.

Mange M.A., Morton A.C., 2007. Geochemistry of heavy minerals. In: Mange, M.A.,Wright, D.T. (Eds.), Heavy Minerals in Use. Developments in Sedimentology 58, 345-391, Elsevier, Amsterdam.

Manzotti P., Ballèvre M., 2013. Multistage garnet in high-pressure metasediments: Alpine overgrowths on Variscan detrital grains. Geology 4, 1151-1154.

Méres Š., 2008. Garnets - important information resource about source area and parental rocks of the siliciclastic sedimentary rocks. In: Conference "Cambelove DNI 2008". Abstract Book, Univerziya Komenského V Bratislava, 37-43 (in Slovak with English abstract).

Méres Š., Hovorka D., 1991. Geochemistry and metamorphic evolution of the Kohút crystalline complex micaschists (the Western Carpathians). Acta Geologica et Geographica Universitatis Comenianae Geologica 47, 15-66.

Perrone V., Martin-Algarra A., Critelli S., Decandia F.A ., D'errico M., Estevez A., Iannace A., Lazzarotto A., Martin-Martin M., Martin-Rojas I., Mazzoli S., Messina A., Mongelli G., Vitale S., Zaghloul N.M., 2006. "Verrucano" and "Pseudoverrucano" in the central-western Mediterranean Alpine chains. In Chalouan A., Moratti G. (Eds.), Geology and active tectonics of the western Mediterranean region and North Africa. Geological Society, London, Special Publication 262, 1-43.

Pett T.K., 2006. Garnetites of the Cardigan Pluton - Evidence for restite and implications for source rock compositions. Master thesis, Bringham Young University, Utah.

Rudnick R.L., Gao S.X., 2003. Composition of the continental crust. In: Rudnick R.L. (Ed.), Treatise on Geochemistry, Volume 3, Elsevier Science, 1-64.

Selyatitskii A,Y., Reverdatto V.V., 2014. Protoliths of UHP garnetites associataed with diamond-bearing rocks near Kumdv-Kol Lake (Kokchetav Massif, Northern Kazakhstan). Doklady Earth Sciences 459, 1423-1428.

Scarciglia F., Critelli S., Borrelli L., Coniglio S., Muto F., Perri F., 2016. Weathering profiles in granitoid rocks of the Sila Massif uplands, Calabria, southern Italy: new insights into their formation processes and rates. Sedimentary Geology 336, 46-67.

SONAREM (Société Nationale De la Recherche Minière), 1980 Projet Edough; Unpublished Data.

Spry P.G., Heimann A., Messerly J.D., Houk R.S., Teale G.S., 2004. Discrimination of metamorphic and metasomatic processes at the Broken Hill lead-zinc-silver deposit, Australia: Rare Earth Element signatures of garnet in garnet-rich rocks, Denver Annual Meeting Geological Society of America, Abstracts 36, 445.

Win K.S., Takeuchi M., Iwakiri S., Tokiwa T., 2007. Provenance of detrital garnets from the Yukawa Formation, Yanase district, Shimanto belt, Kii Peninsula, Southwest Japan. Journal of the Geological Society of Japan 113, 133-145.

Whitney D.L, Evans B.W., 2010. Abbreviations for names of rock-forming minerals. American Mineralogist 95, 185-187.

Yang P., Rivers T., 2001. Chromium and manganese zoning in pelitic garnet and kyanite: spiral, overprint and oscillatory (?) zoning patterns and the role of growth rate. Journal of Metamorphic Geology 19, 455-474.

Zuleger E., Erzinger J., 1988. Determination of REE and Y in silicate materials with ICP-AES. Fresenius' Zeitschrift für Analytische Chemie 332, 140-143.